

NEAR-INFRARED SEARCH FOR C IV ABSORPTION COUNTERPARTS ALONG THE LINE-OF-SIGHTS TO PAIR QUASARS^{1,2}

TORU MISAWA³, NOBUNARI KASHIKAWA^{4,5}, YUICHI OHYAMA⁶, TETSUYA HASHIMOTO⁷ AND
 MASANORI IYE^{4,5,7}
To appear in the Astronomical Journal

ABSTRACT

We carried out a Subaru and UKIRT near infrared imaging survey for H α emitting galaxies around two pair quasar systems (Q0301-005/Q0302-003 and Q2343+125/Q2344+125), and a triple quasar system (KP76/KP77/KP78). Narrow band near infrared filters covering the H α emission expected for galaxies at the confirmed C IV absorption redshift toward the quasar systems were used for this survey. These quasar pairs or triplet are separated at most by 17 arcmins ($\sim 5h^{-1}$ Mpc in proper distance) from each other on the sky, and have common C IV absorption lines at almost identical redshifts at $z = 2.24 - 2.43$, which suggests there could be a Mpc-scale absorbing systems such as a cluster, or a group, of galaxies that cover all the line-of-sights to the pair/triple quasars. Using narrow-band deep images, we detected five candidates for H α emitting galaxies around two of the six fields, Q2343+125 and Q2344+125, whose apparent star formation rates are, extremely high, $20 - 466 \text{ M}_{\odot} \text{ yr}^{-1}$. However, all or most of them are not likely to be galaxies at the absorption redshift but galaxies at lower redshift, because of their extreme brightness. In the fields of the other quasars, we detected no star-forming galaxies, nor did we find any number excess of galaxy counts around them. This no-detection results could be because the luminosities and star formation rates of galaxies are lower than the detection limits of our observations ($K' > 21$ and $SFR < 1.8-240h^{-2}\text{M}_{\odot} \text{ yr}^{-1}$). They could be located outside of the observed field around Q0301 and Q0302, since our targeting field covers only 2% of this pair quasar field. But this is not the case for the other pair/triple quasar fields, because we got effectively large field coverage fractions ($\sim 33 - 75\%$). Otherwise, most C IV absorption lines could be ascribed not to cluster of galaxies, but to isolated star forming pockets far from bright galaxies and could be analogous objects to weak Mg II absorbers.

Subject headings: quasars: absorption lines — galaxies: evolution — quasars: individual (Q0301-005, Q0302-003, KP76, KP77, KP78, Q2343+125, Q2344+125)

1. INTRODUCTION

Several quasars, which are separated from each other on the sky by a few arcmins, have sometimes common metal absorption lines at almost identical redshifts (e.g., Shaver, Boksenberg, & Robertson 1982; Jakobsen et al. 1986; Crotts & Fang 1998). The presence of such common metal absorption lines implies that Mpc-scale gas clouds exist at the redshift, and that they are covering both lines of sight to the quasars. Since it is difficult to assume that a single homogeneous Mpc scale absorber covers both the lines of sight to those quasar pairs based on the framework of the prevalent CDM dominant universe, these metal lines could be produced by gas clouds that are clustering and forming Mpc-scale system (e.g., clouds in galaxies that are members of a Mpc-scale cluster (group) of galaxies). Francis & Hewett (1993) estimated the probability of having strong Ly α absorption lines (i.e., analogue of metal lines) at almost same redshift in two lines of sight separated by a few arcmins is an order of 10^{-4} . If there is a cluster (group) of galaxies, the probability would be increased. Although

several high- z cluster of galaxies have recently discovered, it is still observationally difficult to detect emission lines of star forming galaxies in the redshift desert at $z > 1.5$. However, observations around pair quasars with common metal absorption systems are quite promising (e.g., Francis et al. 1996). High- z cluster of galaxies are excellent targets to investigate star formation histories.

To date, several cluster (group) of galaxies have been detected at $z > 2$. They are often detected around radio-loud quasars or radio galaxies. Pentricci et al. (2000) found 14 Ly α emitting galaxies within the projected distance of 1.5 Mpc from the powerful radio galaxy Q1138-262 at $z=2.16$. Pascarelle et al. (1996) also detected two Ly α emitting galaxies at $z \sim 2.39$ in the field around the weak radio galaxy, 53W002, and also confirmed them spectroscopically. There are several other candidates for cluster (group) of galaxies at $z > 2$ discovered by narrow-band (NB) imaging observations (e.g., LeFèvre et al. 1996, Hu & McMahon 1996). Not only Ly α but H α and [O III] are also useful lines for identification of star forming galaxies

¹ Based on data collected at Subaru Telescope, which is operated by the National Astronomical Observatory of Japan

² Based on data collected at The United Kingdom Infrared Telescope, which is operated by the Joint Astronomy Centre on behalf of the U.K. Particle Physics and Astronomy Research Council.

³ Department of Astronomy and Astrophysics, Pennsylvania State University, 525 Davey Lab, University Park, PA 16802; misawa@astro.psu.edu

⁴ National Astronomical Observatory, 2-21-1 Osawa, Mitaka, Tokyo 181-8588, Japan

⁵ Department of Astronomical Science, The Graduate University for Advanced Studies, 2-21-1 Osawa, Mitaka, Tokyo 181-8588, Japan

⁶ Department of Infrared Astrophysics, Institute of Space and Astronautical Science, Japan Aerospace Exploration Agency, 3-1-1 Yoshinodai, Sagami-hara, Kanagawa, 229-8510, Japan

⁷ Department of Astronomy, School of Science, University of Tokyo, 7-3-1 Hongo, Bunkyo-ku, Tokyo 113-0033 Japan

(e.g., Teplitz, Malkan, & McLean 1998; Iwamuro et al., 2000). Galaxies have also been discovered in the fields around quasars as counterparts of strong absorption systems. C IV absorption systems with W_{rest} (rest-frame equivalent width) $> 0.4 \text{ \AA}$ and Mg II absorption systems with $W_{rest} > 0.3 \text{ \AA}$ are thought to have ~ 70 and ~ 40 kpc sizes around L^* galaxies, by comparing Press-Schechter function (as luminosity function of galaxy) and the number densities of these absorption systems per redshift. Charlton & Churchill (1996) showed that both spherical halo and randomly oriented disks with only 70–80% covering factors of gas clouds can recover the observed properties of Mg II absorbers, by performing a Monte Carlo simulation. This means that the distribution of the Mg II absorbers around galaxies are not smooth but patchy. There are some galaxy surveys around *single* quasars (e.g., Bergeron & Boisse 1991; Steidel, Dickinson, & Persson 1994; Lanzetta et al. 1998; Chen & Lanzetta 2001; Chen et al. 2001). However, for *pair* quasar regions, only a few observations have been carried out based on common metal absorption lines of pair quasars (e.g., Teplitz et al., 1998; Francis, Woodgate, & Danks 1997; Francis et al., 1996), in spite of its high potential.

In this paper, we report the results of our near-infrared (NIR) *NB* imaging survey of the fields around pair/triple quasars that have common metal absorption lines at $z \sim 2.3$. They are separated at most by 17 arcmins ($\sim 5h^{-1}$ Mpc in proper distance, with $h=H_0/72 \text{ km s}^{-1} \text{ Mpc}^{-1}$). Our objectives are to search for star forming galaxies that produce the common metal absorption lines, and see if there are galaxies that are member of the cluster (or group) of galaxies including those star forming galaxies.

We present the outline of the observations and data reduction in § 2, and the brief description of the photometric analysis in § 3. In § 4, we present the result for each quasar field. We summarize and discuss our results in § 5. Throughout this paper, we assume $H_0=72 \text{ km s}^{-1} \text{ Mpc}^{-1}$, $\Omega_0 = 0.3$, $\Omega_\Lambda = 0.7$, and $q_0=0.5$.

2. OBSERVATION AND DATA REDUCTION

We observed the fields of pair/triple quasars. These quasars have common absorption systems (at least contain C IV doublets in them) with small redshift difference, $\Delta z \sim 0.005$, which corresponds to velocity difference, $\Delta v \sim 500 \text{ km s}^{-1}$, in the frame of the absorbers. However, we should notice that if redshift difference is caused by the Hubble flow, these absorbers would be separated by much larger than the typical size of cluster of galaxies along the line of sight. We chose *NB* filters which cover redshifted H α emission lines. Filter name, central wavelength, band width, corresponding redshift for H α emission line detection, and the bandpass ratio of *NB* to broad-band (K' -band), are listed in Table 1. To see the color excess, we also carried out K' -band imaging observations. The observations were performed with either the Cooled Infrared Spectrograph and Camera for OHS (CISCO; Motohara et al. 1998) on the Subaru Telescope (Iye et al. 2004), or UKIRT First-Track Imager (UFTI; Roche et al. 2002) on the UKIRT. Both instruments have HAWAII 1024 \times 1024 pixel HgCdTe arrays that cover a field of view (FoV) of $108'' \times 108''$ and $92'' \times 92''$, respectively. We summarize the observation logs in Table 2; columns (1) and (2) are

quasar name and its emission redshift. Absorption redshift of common metal lines is given in column (3). Identified ion transition is listed in column (4). The data was taken on the date in column (6) using the filter in column (5). Exposure time and average seeing size are in columns (7) and (8). Columns (9) and (10) are detection limit with 3σ and 5σ levels, which are magnitudes of the faintest artificial objects that are placed in the observed frame and extracted with 3σ or 5σ detection level. We will describe the simulation in detail in § 3. In columns (11) and (12) we also present 3σ detection limits of H α emission line and correspondent star formation rate. References of spectroscopic observations are given in column (13).

Data reduction was processed in a standard manner with IRAF. All objects are identified by the Source Extractor program (Bertin & Arnouts 1996) with detecting-threshold of 2.0σ . We evaluated the magnitudes of objects in circular apertures twice as large as seeing size.

3. PHOTOMETRIC ANALYSIS

In the color-magnitude (CM) analysis to isolate H α emitting objects, we need an accurate evaluation of the photometric errors. Therefore we have created 10,000 artificial stars with the seeing size of each frame. Their magnitude distribution is homogeneous between $K' = 15$ –22 mag. We placed them in both K' and *NB* frames randomly. We plot CM diagrams to compare the detected objects against the simulated artificial objects. The candidates for intervening galaxies at $z \sim 2.3$ have $K' - NB$ color excess because their H α emission lines are redshifted into the *NB* filter bandpass, which makes them deviated from the distributions of the artificial objects. We regard all the objects as candidates of H α emitters, if they are deviated toward the positive direction in the vertical axis (i.e., $K' - NB$) more than 3σ from the distribution of the artificial objects in CM diagrams. It is unlikely that the color excess is caused by other lines whose rest-frame wavelength are shorter than H α , such as Ly α , [O II], or [O III] lines, because galaxies should be at $z \sim 17.5$, 5.0, and 3.5 if these lines are redshifted into the bandpass of *NB* filters. Flux of these objects would be too weak to detect in our observations. On the other hand, if candidate objects are much brighter than the typical magnitudes of H α emitting galaxies that produce metal absorption lines; $J \sim 22.5$, $H \sim 21.5$, and $K \sim 20.8$ (Teplitz et al. 1998), these color excess could be due to near-infrared emission lines from galaxies at lower redshift, such as [Fe II]1.257 μ , [Fe II]1.644 μ , Pa α , Pa β , and Br γ , which is described in § 5.

If we assume that the color excess is attributed to H α emission lines, we can estimate the flux of H α line from the K' and *NB* magnitudes by

$$K' - NB = 2.5 \log \left(1 \pm 10^{\frac{K' - NB}{2.5}} \right) + K'_0 - NB_0, \quad (1)$$

where K'_0 and NB_0 are magnitude zeropoints (i.e., a magnitude corresponding to the flux, one count per second on each pixel) for K' and *NB* filters (e.g., Iwamuro et al. 2000). Here, the constant, γ , is defined as follows,

$$\gamma = K'_0 - 2.5 \log \left(\frac{f_{H\alpha}}{W_{NB}} \right), \quad (2)$$

where W_{NB} is the band width of the *NB* filter and $f_{H\alpha}$ is a total H α line flux (without the continuum flux) that

is covered by the *NB* filters. We define 1, 2, and 3 σ deviation borders in CM diagram as the equation (1) with fixed γ -value that cover 68.3, 95.5, and 99.7 % of all the artificial objects.

From the luminosity of $H\alpha$ emission line, $L_{H\alpha}$ (ergs s^{-1}), we can also evaluate star formation rate (*SFR*) using the conversion relation described in Kennicutt (1998),

$$SFR_{H\alpha} (total) = \frac{L_{H\alpha}}{1.27 \times 10^{41} \text{ ergs } s^{-1}} M_{\odot} \text{ yr}^{-1}, \quad (3)$$

where we assume the Salpeter initial mass function with lower and upper mass cutoffs of 0.1 and 100 M_{\odot} .

4. RESULTS

The color-magnitude analysis of all the objects detected in the six fields around pair/triple quasars yielded two and three candidates for star forming galaxies around Q2343+125 and Q2344+125, respectively. In this section, we describe the result for each quasar field.

4.1. KP76/KP77/KP78

The quasar triplet (KP76:Q1623+2651A at $z_{em} = 2.467$, KP77:Q1623+2653 at $z_{em} = 2.526$, and KP78:Q1623+2651B at $z_{em} = 2.605$) is located on the sky within a small FoV of 3 arcmin: 147'' between KP76 and KP77, 127'' between KP76 and KP78, and 177'' between KP77 and KP78 (e.g., Crotts & Fang 1998). All of them have C IV absorption lines at $z \sim 2.24$ in their spectra with total equivalent widths, $W_{rest} \sim 0.14, 0.08$, and 2.34 Å, respectively. Other transitions of metal lines such as C I, C II, Si II, Si III, Si IV, N V are also identified. The radial velocity separations of these absorption lines are within 500 km s^{-1} of each other in the frame of the absorbers. The linear angular distance on the sky between these systems corresponds to $\sim 1h^{-1}$ Mpc at $z \sim 2.24$, which is comparable to the typical size of cluster of galaxies in the local universe.

We carried out two deep imaging observations of the fields around KP76 with UKIRT + UFTI with FoV of $90'' \times 90''$ (i.e., $500h^{-1}$ kpc \times $500h^{-1}$ kpc), and KP77/KP78 with Subaru + CISCO with FoV of $108'' \times 108''$ (i.e., $600h^{-1}$ kpc \times $600h^{-1}$ kpc). Although we found two objects around KP76 that were detected only in *NB* filters, they are confirmed to be ghost images of brightest sources in the frames. There are not any other candidates for star forming galaxies with $SFR > 6.8h^{-2} M_{\odot} \text{ yr}^{-1}$ ($f_{H\alpha} > 2.4 \times 10^{-17}$ ergs $s^{-1} \text{ cm}^{-2}$) in KP76 field or $SFR > 1.8h^{-2} M_{\odot} \text{ yr}^{-1}$ ($f_{H\alpha} > 6.3 \times 10^{-18}$ ergs $s^{-1} \text{ cm}^{-2}$) in KP77/KP78 field, with 3σ detection limit of $K' \leq 21$.

4.2. Q0301-005/Q0302-003

This pair quasar is separated by about 17' from each other on the sky, which corresponds to $\sim 5.5h^{-1}$ Mpc at $z \sim 2.43$ (e.g., Dobrzycki & Bechtold 1991). They have common C IV and/or Si IV doublets at $z \sim 2.96, 2.72$, and 2.43 (Cowie et al., 1995; Songaila 1998; Steidel 1990), of which only $H\alpha$ emissions at $z \sim 2.43$ can be identified by the *NB* filter of our observation. We took two images with UKIRT + UFTI around both quasars by putting them at the centers of frames. We identified no candidates for star forming galaxies with $SFR > 236h^{-2} M_{\odot} \text{ yr}^{-1}$ ($f_{H\alpha} > 6.9 \times 10^{-16}$

ergs $s^{-1} \text{ cm}^{-2}$) in Q0301 field and $SFR > 23h^{-2} M_{\odot} \text{ yr}^{-1}$ ($f_{H\alpha} > 6.7 \times 10^{-17}$ ergs $s^{-1} \text{ cm}^{-2}$) in Q0302 field. The 3σ detection limits are $K' = 20.1$ around Q0301-005 and $K' = 21.1$ around Q0302-003.

4.3. Q2343+125/Q2344+125

Q2343+125 has C IV absorption lines at $z=2.4285$ and 2.4308, while Q2344+125 has corresponding strong C IV absorption lines at $z=2.4265$ and 2.4292 (Sargent, Boksenberg, & Steidel 1988). The velocity separation of these absorption lines along the line of sight is smaller than 400 km s^{-1} . These quasars are separated from each other only by 5' ($\sim 1.6h^{-1}$ Mpc) at $z \sim 2.43$. The C IV absorption system in Q2343+125, which was classified as Damped Ly α system (Lu, Sargent, & Barlow 1998), has other metal lines such as Al II $\lambda 1670$, Fe II $\lambda 1608$, Si II $\lambda 1526$.

To date, several deep imaging observations have been carried out for this field. Bergvall et al. (1997) took an optical narrow-band deep images to search Ly α emitting objects around both of the quasars, but did not find any candidates. Ly α emissions, however, are strongly affected by dust extinction, which makes it difficult to detect. Therefore, Teplitz et al. (1998) took deep NIR images with a small FoV ($38'' \times 38''$) around Q2343+125 to search $H\alpha$ emitters, but nothing was detected. Bunker et al. (1999) also carried out a long-slit K-band spectroscopic search for $H\alpha$ emitters in the vicinity (within $11'' \times 2.5''$) of Q2343+125, but found nothing above 3σ limit ($f_{H\alpha} = 6.5\text{--}16 \times 10^{-17}$ ergs $s^{-1} \text{ cm}^{-2}$).

In our NIR images taken with Subaru + CISCO, we detected two candidates (objects A and B) for star forming galaxies at $z \sim 2.43$ around Q2343+125 (Figure 1) and three candidates (objects C, D, and E) around Q2344+125 (Figures 2), whose K' magnitude, $H\alpha$ flux, and *SFR* are listed in Table 3, by assuming that they are actually galaxies at $z \sim 2.43$. Unfortunately, it is difficult to tell the morphological type of the identified objects because of low spatial resolutions in the observed images. The 3σ detection limits of these images are $K' = 20.5$ and 21.1, respectively. These objects were outside of the frame (or just at the borders of FoV) in the previous observation by Teplitz et al. (1998). The CM diagrams are also presented in Figures 3 and 4. All candidates are bright ($K' < 18.3$) and their apparent *SFRs* are very large ($> 20h^{-2} M_{\odot} \text{ yr}^{-1}$). We will discuss them in the next section.

5. SUMMARY AND DISCUSSION

We detected five candidates (objects A – E) for intervening galaxies around two of six pair/triple quasar fields, by NIR *NB* imaging observations. They are all bright ($K' < 18.3$) with large $H\alpha$ fluxes ($f_{H\alpha} > 5.7 \times 10^{-17}$ ergs $s^{-1} \text{ cm}^{-2}$).

Teplitz et al. (1998) detected 13 $H\alpha$ emitters, using same method to ours, of which the brightest two objects ($K'=15.42$ with $f_{H\alpha} = 249 \times 10^{-17}$ ergs $s^{-1} \text{ cm}^{-2}$ around Q0114-089 and $K'=18.15$ with $f_{H\alpha} = 581 \times 10^{-17}$ ergs $s^{-1} \text{ cm}^{-2}$ around PC2149+0221) have similar properties to ours. Teplitz et al. (1998) regarded them as Seyfert I galaxies, because they are extremely compact and one of them had broad emission lines. However, all (or at least substantial fraction) of our objects with absolute magnitude, $M_B < -24+5\log h$, are not likely to be

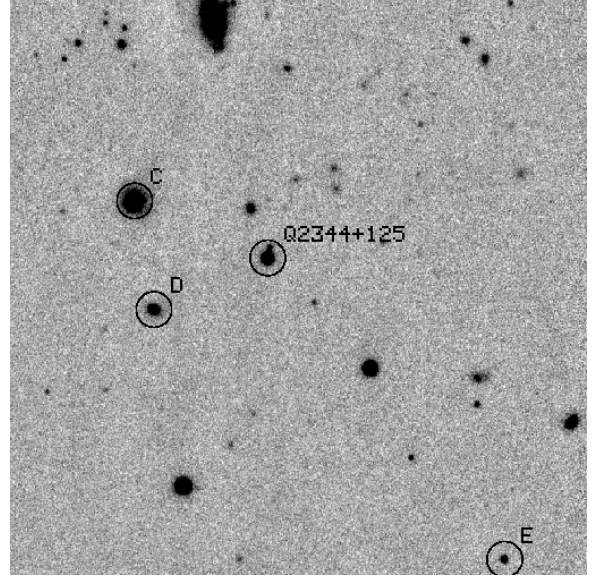
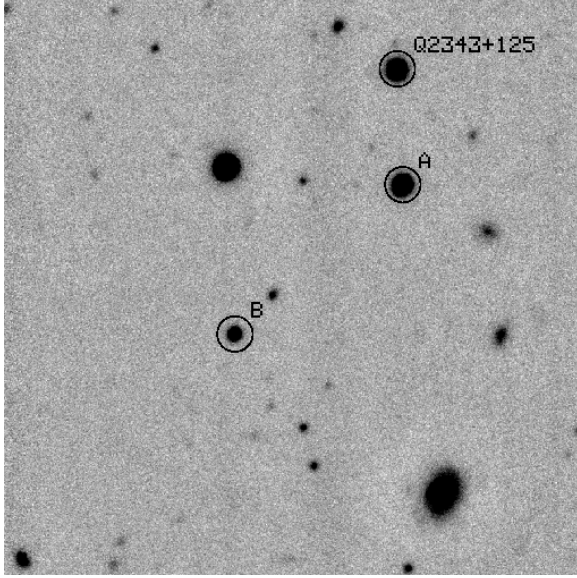


FIG. 1.— (Left) K' image of the field around Q2343+125. The quasar and 2 objects that have color excess in NB filter are surrounded by circles. FoV of the images is $94''.5 \times 94''.5$ (slightly trimmed from the observed image), which corresponds to $512h^{-1} \text{ kpc} \times 512h^{-1} \text{ kpc}$ at $z \sim 2.43$.

FIG. 2.— (Right) Same as Figure 1, but for the field around Q2344+125.

Seyfert galaxies at $z \sim 2.43$, because their volume density¹ ($\sim 5.2h^3 \text{ Mpc}^{-3}$) is much larger than the global density of AGNs with similar luminosities at similar redshift ($\sim 10^{-6} \text{ Mpc}^{-3}$; Warren, Hewett, & Osmer 1994). Some

of them could be foreground (active) galaxies at $z \sim 0.04, 0.20, 0.37, 0.76$, and 0.79 , whose $\text{Br}\gamma$, $\text{Pa}\alpha$, $[\text{Fe II}]1.644\mu$, $\text{Pa}\beta$, and $[\text{Fe II}]1.257\mu$ emission lines are redshifted into the bandpass of NB filters. These are most prominent

¹ We evaluated this value by assuming that all five objects exist within $1.6h^{-1} \text{ Mpc}$ from each other along line of sight, which is consistent to the separation of the lines of sight to the pair quasars at $z \sim 2.43$.

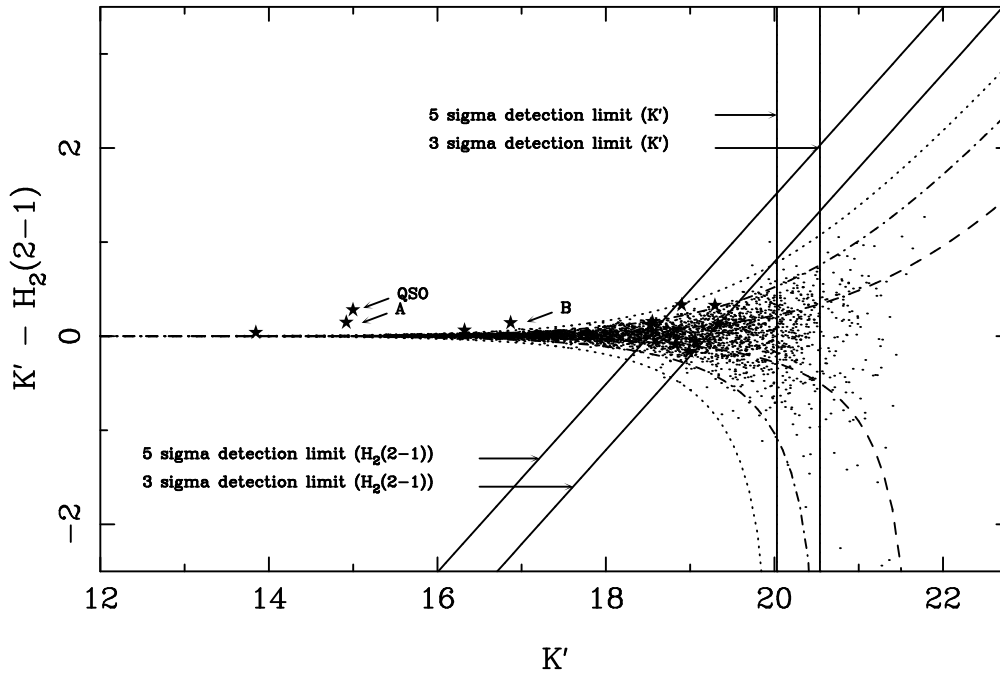


FIG. 3.— $K' - NB$ ($H_2(2-1)$) color versus K' diagram for the field around Q2343+125. The filled stars denote the objects detected in both K' and NB images, while the thin dots represent the simulated data (only one of every ten data are plotted to make them easy to see). The three marked objects are a quasar and candidates for $H\alpha$ emitting galaxies at $z \sim 2.43$. Dashed, dot-dashed, and dotted curves are 1, 2, and 3 σ deviations of the artificial objects placed in CM diagram. Solid lines denote 3 σ and 5 σ detection limits in K' and NB frames.

emission lines of active galaxies in *NIR* window (e.g., Simpson et al. 1996; Kawara, Nishida, & Taniguchi 1988; Goodrich, Veilleux, & Hill 1994). Actually, Tamura et al. (2001) found a galaxy at $z=0.132$ whose $P\alpha$ is strong, $f_{P\alpha} = 3.4 \times 10^{-17}$ ergs s $^{-1}$ cm $^{-2}$ by *NB* imaging observation. Thus, it seems unlikely that there exists cluster (group) of bright galaxies at $z \sim 2.43$.

In the fields of other pair/triple quasars, we detected no galaxies at redshifts of the common C IV absorption lines. There are at least four possible reasons as follows.

First, this could be because the star formation rates are too low to detect in the observed frames. The minimum *SFR* and H α flux we can detect in each observed frame is described in the previous section and summarized in Table 2. Typical *SFR*s of individual field galaxies at $z \sim 2$ have been estimated to be $\sim 10\text{--}35 M_{\odot} \text{ yr}^{-1}$ (without dust extinction correction) by infrared imaging surveys with narrow-band filters and spectroscopic observations (e.g., Moorwood et al. 2000; Iwamuro et al. 2000). Similar *SFR* is derived for Lyman break galaxies at $z \sim 2\text{--}3$, from spectroscopic observation based on H β emission lines ($\sim 20\text{--}70 M_{\odot} \text{ yr}^{-1}$) with one exception ($\sim 270 M_{\odot} \text{ yr}^{-1}$) (Pettini et al. 1998). Juneau et al. (2005) also estimated *SFR*s of field galaxies at $z \sim 2$ from UV continuum luminosities with dust extinction correction, and again got similar values ($\sim 30 M_{\odot} \text{ yr}^{-1}$). Teplitz et al. (1998) searched star forming galaxies at same redshift as metal absorption systems, and found 11 H α emitters at $z = 2.3\text{--}2.5$ within 250 kpc of quasar lines of sight. Their average *SFR* is $\sim 50 M_{\odot} \text{ yr}^{-1}$. The 3σ detection limits of *SFR* in Q0301/Q0302 fields are comparable or larger than

the average *SFR* at $z \sim 2$ in the literature. In this case, star forming galaxies could not be detected unless they have extremely large *SFR*s. On the other hand, image depths of the other fields are enough to detect field star forming galaxies with typical *SFR*s, which means that absorbers corresponding to C IV absorption lines could have lower *SFR*s, compared with field galaxies at same redshift.

Second possible reason of no-detection is that typical star forming galaxies could be faint compared to the detection limits of our observations. At $z \sim 2$, an average K' magnitude of star forming galaxies detected based on metal absorption lines is $K' \sim 20.8$ (Teplitz et al. 1998). On the other hand, of six fields observed, one (or four) fields were observed to provide deep images enough to detect such faint star forming galaxies with the 5σ (or 3σ) detectability. Although observed images are very deep for most of the fields, these could not enough for some fields (i.e., Q0301 and Q2343 fields). We also confirmed that there was no number excess of galaxy counts in the fields around the pair quasars (Figure 5), compared with the global value of field galaxies around Subaru Deep Field (Maihara et al. 2001). Thus, we cannot yet reject existences of cluster (group) of galaxies in our pair/triple quasar fields, because they could contain only faint galaxies with $K' \geq 21$.

Thirdly, it is also possible that our targetting fields did not cover star forming galaxies by chance. We calculated field coverage fractions (i.e., fraction of the area covered by our observations to the area of the pair quasar field²). We got effectively large values as $\sim 75\%$ and 33% for KP76/KP77/KP78 and Q2343/Q2344 fields, respectively,

² This means the area of circles on which all pair/triple quasars are located. For example, this area would be evaluated to be $\pi \times (150'')^2$ for Q2343/Q2344 pair quasars that are separated by $300''$ from each other on the sky. Areas used here are the lower limit of the size of possible cluster (group) of galaxies, because member galaxies probably distribute outside of this circles if they really exist.

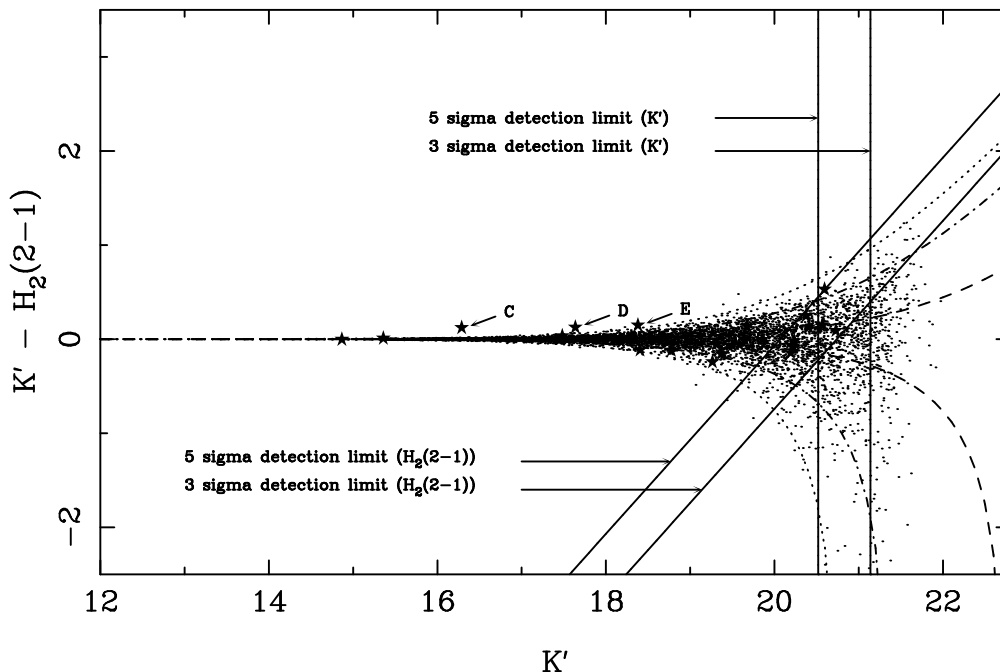


FIG. 4.— Same as Figure 3, but for the field around Q2344+125. Quasar is not plotted, because we do not plot objects blending with neighbors, and that the quasar blends.

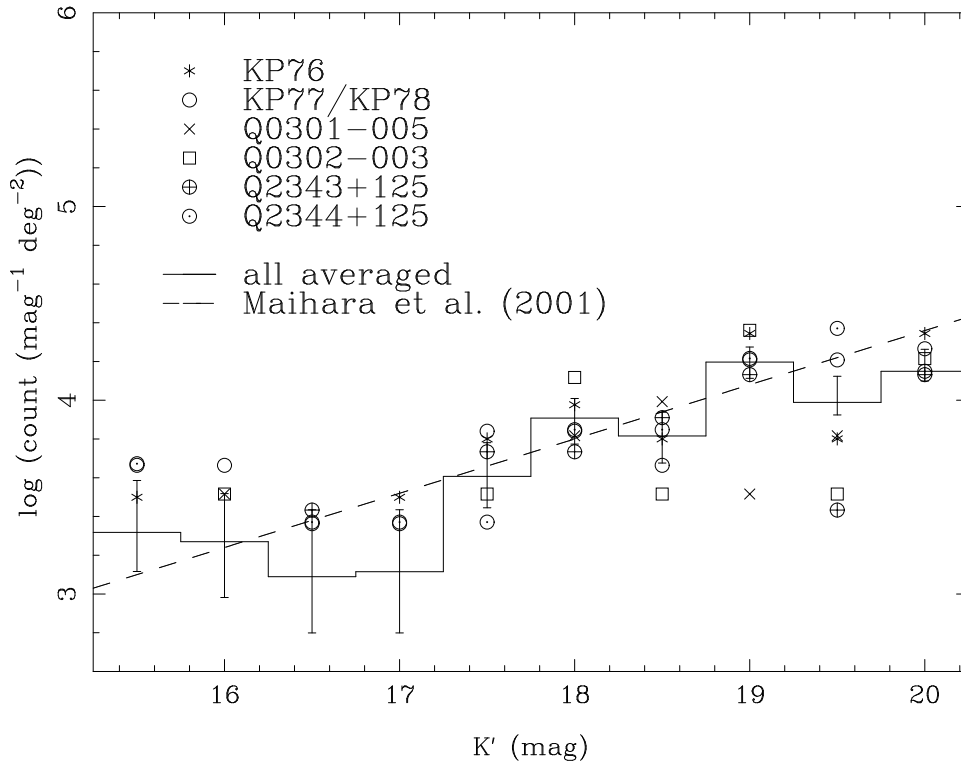


FIG. 5.— Galaxy number count ($\text{mag}^{-1} \text{deg}^{-2}$) vs. K' magnitude in each pair quasar field. We do not plot marks if no objects were found in a given bin of K' magnitude in some quasar fields. Solid line histogram with 1σ error denotes the number counts averaged in all the six fields. We also overlaid the number count of field galaxies evaluated in Subaru Deep Field (Maihara et al. 2001). We adopted *best* magnitude (see Source Extractor program manual; Bertin & Arnouts 1996) in this plot, to compare them directly with the Maihara et al.'s result.

while the coverage fraction for Q0301/Q0302 field is very small, $\sim 2\%$. It seems unlikely that we happened to miss both star forming galaxies and a number excess of galaxies in the fields around KP76/KP77/KP78 and Q2343/Q2344 pair/triple quasars, if cluster of galaxies really exist. In the case of Q0301/Q0302 field, the result is still open to some uncertainties (e.g., coverage fraction could be underestimated, if galaxies are distributed not spherically but filamentally in the scale of $\sim 5\text{Mpc}$ along the pair quasars).

Finally, perhaps, most of C IV lines, whose counterparts were not identified, could arise in star forming pockets outside bright galaxies (e.g., the ejecta of Type Ia supernovae, dwarf galaxies, or low surface brightness galaxies), which have already been suggested as counterparts of weak ($W_{\text{rest}} < 0.3 \text{ \AA}$) Mg II lines (Rigby et al. 2002). These pockets have multiple phases; kiloparsec scale higher ionization phase to produce C IV, and compact scale ($\sim 10\text{pc}$) low ionization phase with high density to produce Mg II (Charlton et al. 2003). The redshift path density of weak Mg II systems is twice of the strong Mg II systems that have almost always corresponding luminous galaxies (Steidel 1995). Weak Mg II systems also have high metallicity; solar or super-solar (Charlton et al. 2003). Nonetheless, corresponding luminous galaxies are rarely found within $\sim 50h^{-1} \text{ kpc}$ of the quasars (Churchill et al. 1999). All the

properties of weak Mg II systems are consistent with the no-detection of star forming galaxies in our observations.

With K -band imaging observations, we placed photometric and SFR upper limits of H α emitters corresponding to C IV absorption lines toward the lines of sight of pair/triple quasars. Deeper imaging surveys for wider fields that cover completely pair/triple quasar fields are necessary before concluding whether galaxy clusterings corresponding to metal absorption lines really exist or not. A large number of multiple quasars also have recently been discovered by the large scale surveys such as Sloan Digital Sky Survey (SDSS; Schneider et al. 2005) and 2dF QSO Redshift Survey (2QZ; Croom et al. 2004), which enable us to extend this survey in the future.

Part of the observation was kindly carried out in the engineering time of Subaru Telescope. We would like to thank J.C. Charlton and M. Eracleous for their comments to develop this study, and I. Tanaka and M. Kajisawa for their useful advices on reduction of infrared data. We also would like to thank D. Tytler and V. D'Odorico for informing us of the coordinate of one of our targets. Finally, we wish to thank the anonymous referee for many helpful comments and suggestions.

REFERENCES

- Bergvall, N., Östlin, G., Karlsson, K. G., Örndahl, E., and Rönnback, J., 1997, *A&A*, 321, 771
 Bergeron, J., and Boissé, P., 1991, *A&A*, 243, 344
 Bertin, E., and Arnouts, S., 1996, *A&AS*, 117, 393
 Bunker, A.J., Warren, S.J., Clements, D.L., Williger, G.M., and Hewett, P.C., 1999, *MNRAS*, 309, 875
 Charlton, J.C., Ding, J., Zonak, S.G., Churchill, C.W., Bond, N.A., Rigby, J.R., 2003, *ApJ*, 589, 111

- Charlton, J. C. and Churchill, C. W., 1996, *ApJ*, 465, 631
- Churchill, C. W., Rigby, J. R., Charlton, J. C., and Vogt, S. S., 1999, *ApJS*, 120, 51
- Chen, H.-W., Lantezza, K. M., and Webb, 2001, *ApJ*, 556, 158
- Chen, H.-W., Lantezza, K. M., Webb, J. K., and Barcons, X., 2001, *ApJ*, 559, 654
- Cowie, L.L., Songaila, A., Kim, T.-S., and Hu, E.M., 1995, *AJ*, 109, 1522
- Croom, S. M., Smith, R. J., Boyle, B. J., Shanks, T., Miller, L., Outram, P. J., and Loaring, N. S., 2004, *MNRAS*, 349, 1397
- Crotts, A. P. S., and Fang, Y., 1998, *ApJ*, 502, 16
- Dobrzycki, A., and Bechtold, J., 1991, *ApJ*, 377, 69
- Francis, P. J., and Hewett, P. C., 1993, *AJ*, 105, 1633
- Francis, P. J., Woodgate, B. E., Warren, S. J., Møller, P., Mazzolini, M., Bunker, A. J., Lowenthal, J. D., Williams, T. B., Minezaki, T., Kobayashi, Y., and Yoshii, Y., 1996, *ApJ*, 457, 490
- Francis, P. J., Woodgate, B., and Danks, A. C., 1997, *ApJ*, 482, 25
- Goodrich, R.W., Veilleux, S., and Hill, G.J., 1994, *ApJ*, 422, 521
- Hu, E.M., and McMahon, R.G., 1996, *Nature*, 382, 231
- Iwamuro, F., Motohara, K., Maihara, T., Iwai, J., Tanabe, H., Taguchi, T., Hata, R., Terada, H., Goto, M., Ohya, S., Iye, M., Yoshida, M., Karoji, H., Ogasawara, R., and Sekiguchi, K., 2000, *PASJ*, 52, 73
- Iye, M., et al., 2004, *PASJ*, 56, 381
- Jakobsen, P., Perryman, M. A. C., Ulrich, M. H., Macchetto, F., and di Serego Alighieri, S., 1986, *ApJ*, 303, 27
- Juneau, S., et al., 2005, *ApJ*, 619, 135
- Kawara, K., Nishida, M., and Taniguchi, Y., 1988, *ApJ*, 328, L41
- Kennicutt, R. C. Jr., 1998, *ARA&A*, 36, 189
- Lanzetta, K. M., Chen, H.-W., Webb, J. K., and Barcons, X., 1998, invited review for IAU Colloquium 171, *The Low Surface Brightness Universe*
- LeFèvre, O.L., Deltorn, J.M., Crampton, D., and Dickinson, M., 1996, *ApJ*, 471, 11
- Lu, L., Sargent, W.L.W., and Barlow, T.A., 1998, *AJ*, 115, 55
- Maihara, T. et al., 2001, *PASJ*, 53, 25
- Moorwood, A.F.M., van der Werf, P.P., Cuby, J.G., and Oliva, E., 2000, *A&A*, 362, 9
- Motohara, K., et al., 1998, in *Proc. SPIE 3354: Infrared Astronomical Instrumentation*, ed. A. M. Fowler, 659
- Pascarelle, S.M., Windhorst, R.A., Driver, S.P., Ostrander, E.J., and Keel, W.C., 1996, *ApJ*, 456, 21
- Pentricci, L., Kurk, J. D., Röttgering, H. J. A., Miley, G. K., van Breugel, W., Carilli, C. L., Ford, H., Heckman, T., McCarthy, P., and Moorwood, M., 2000, *A&A*, 361, L25
- Pettini, M., Kellogg, M., Steidel, C.C., Dickinson, M., Adelberger, K.L., and Giavalisco, M., 1998, *ApJ*, 508, 539
- Rigby, J.R., Charlton, J.C., and Churchill, C., 2002, *ApJ*, 565, 743
- Roche P.F. et al. 2002, *Proc Spie* 4841, *Instrument Design and Performance for Optical/IR Ground-Based Telescopes*, eds. M Iye and A.F Moorwood
- Sargent, W.L.W., Boksenberg, A., and Steidel, S.S., 1988, *ApJS*, 68, 539
- Schneider, D. P., et al., 2005, *astro-ph/0505679*
- Shaver, P. A., Boksenberg, A., and Robertson, J. G., 1982, *ApJ*, 261, 7
- Simpson, C., Forbes, D.A., Baker, A.C., and Ward, M.J., 1996, *MNRAS*, 283, 777
- Smette, A., Robertson, J.G., Shaver, P.A., Reimers, D., Wisotzki, L., and Koehler, T., 1995, *A&AS*, 113, 199
- Songaila, A., 1998, *AJ*, 115, 2184
- Steidel, C.C., 1995, in *QSO Absorption Lines*, ed. G. Meylan (Garching: Springer Verlag), 139
- Steidel, C. C., Dickinson, M., and Persson, S. E., *ApJ*, 437, 75
- Steidel, C.C., 1990, *ApJS*, 74, 37
- Teplitz, H.I., Malkan, M., and McLean, I. S., 1998, *ApJ*, 506, 519
- Tamura, N., Ohta, K., Maihara, T., Iwamuro, F., Motohara, K., Takata, T., and Iye, M., 2001, *PASJ*, 53, 653
- Warren, S. J., Hewett, P. C., and Osmer, P. S., 1994, *ApJ*, 421, 412

TABLE 1
TRANSMISSION OF NARROW BAND FILTERS

(1) Filter	(2) λ_{cen}^a (μm)	(3) $\Delta\lambda^b$ (μm)	(4) $z(H\alpha)^c$	(5) $\Delta\lambda_{NB}/\Delta\lambda_{K'}^d$ (%)
2.122 ^e	2.119	0.031	2.229	9.1
2.248S ^e	2.253	0.035	2.433	10.3
$H_2(2-1)^f$	2.250	0.022	2.428	6.9
$H_2(1-0)^f$	2.120	0.020	2.230	6.3

^aCentral wavelength of the filter.

^bBandpass width of the filter with 50 % transmission.

^cRedshift of a star-forming galaxy whose $H\alpha$ emission line is redshifted into the center of the filter.

^dBandpass ratio of narrow-band to K' band filters in percent.

^eFilter available with UKIRT+UFTI.

^fFilter available with Subaru+CISCO.

TABLE 3
CANDIDATES FOR $H\alpha$ EMITTERS

(1) Field	(2) Object	(3) K' (mag)	(4) $f_{H\alpha}^a$ ($\text{ergs s}^{-1} \text{cm}^{-2}$)	(5) SFR ^b ($h^{-2}M_{\odot} \text{yr}^{-1}$)	(6) FWHM ($''$)
Q2343+125	A	14.92	1.35×10^{-15}	466	0.97
	B	16.87	2.17×10^{-16}	75	0.99
Q2344+125	C	16.29	3.14×10^{-16}	108	0.82
	D	17.64	9.34×10^{-17}	32	0.80
	E	18.28	5.67×10^{-17}	20	0.65

^aTotal flux of $H\alpha$ emission line, without a correction for the effects of $[\text{N II}]$ line.

^bStar formation rate in unit of solar-mass per year.

TABLE 2
OBSERVATION LOG

(1) QSO	(2) z_{em}	(3) z_{abs}	(4) Ion	(5) Filter	(6) Date	(7) Exposure (sec)	(8) Seeing ($''$)	(9) 3σ (mag)	(10) 5σ (mag)	(11) $f_{H\alpha}(lim.)^a$ ($\text{ergs s}^{-1} \text{cm}^{-2}$)	(12) $\text{SFR}(lim.)^b$ ($h^{-2} \text{M}_{\odot} \text{yr}^{-1}$)	(13) Reference
KP76 ^c	2.467	2.2462	C IV, Si IV	K98	May 24–25 2002	11760	0.42	21.39	21.03	2.4×10^{-17}	6.8	1
				2.122	May 24–25 2002	33100	0.42	20.91	20.39			
KP77/KP78 ^d	2.526,2.605	2.2445,2.2417	C IV, Si IV	K'	May 14 2003	1440	0.40	21.09	20.42	6.3×10^{-18}	1.8	1
				$H_2(1-0)$	May 14 2003	5760	0.39	20.00	19.34			
Q0301–005 ^c	3.223	2.4291	C IV, Si IV	K98	Dec 22–23 2002	4860	0.82	20.06	19.34	6.9×10^{-16}	236	2
				2.248S	Dec 22–23 2002	11700	0.88	18.77	18.14			
Q0302–003 ^c	3.285	2.4233	C IV, Si IV	K98	Dec 22 2002	4860	0.48	21.07	20.44	6.7×10^{-17}	23	2
				2.248S	Dec 22 2002	12600	0.50	20.15	19.59			
Q2343+125 ^d	2.515	2.4285,2.4308	C IV	K'	Nov 19 2000	3260	0.94	20.54	20.03	1.6×10^{-17}	5.5	3
				$H_2(2-1)$	Nov 19 2000	8640	0.93	19.21	18.51			
Q2344+125 ^d	2.763	2.4265,2.4292	C IV	K'	Nov 7 2003	1920	0.52	21.14	20.52	9.3×10^{-18}	3.2	3
				$H_2(2-1)$	Nov 7 2003	5760	0.52	20.74	20.07			

^a 3σ detection limit of $H\alpha$ emission line.

^b 3σ detection limit of star formation rate.

^cObserved with UKIRT + UFTI.

^dObserved with Subaru + CISCO.

References. — (1) Crotts & Fang 1998; (2) Steidel 1990, Cowie et al. 1995; Dobrzycki & Bechtold 1991; (3) Teplitz et al. 1998